

Fabrication and Characterization of $\text{LiNO}_3\text{-Al}_2\text{O}_3$ Composite Solid Electrolytes

M. Sulaiman^{1,2}, A. A. Rahman¹ and N. S. Mohamed¹

¹ Centre for Foundation Studies in Science, University of Malaya, 50603 Kuala Lumpur, Malaysia

² Institute of Graduate Studies, University of Malaya, 50603 Kuala Lumpur, Malaysia

Abstract. Composite solid electrolytes $(1-x)\text{LiNO}_3\text{-}x\text{Al}_2\text{O}_3$ with $x = 0.1\text{-}0.5$ are prepared via water based sol gel method followed by calcinations at 150°C . Conductivity, thermodynamic and structure properties of the composites are investigated. The composites are characterized by X-ray diffraction, differential scanning calorimeter, scanning electron microscopy and energy dispersive X-ray analyses. The ionic conductivity study is carried out by impedance spectroscopy. The XRD and DSC results show an amorphous characteristic of LiNO_3 in the composite system. SEM micrographs reveal an excellent interfacial contact between the amorphous phases. This includes the spreading of the ionic salt over the alumina surfaces. The composite sample with $x = 0.3$ is found to have a mesoporous structure constructed by many interconnected of lithium nitrate, alumina and lithium aluminate which are identified by the EDX analysis. Ionic conductivity study shows that the amorphous phase of LiNO_3 influences the ionic transport in the composite solid electrolytes. The conductivities of the composites obtained are in the order of $\sim 10^{-4}$ and $\sim 10^{-3}$ S cm^{-1} at room temperature and 180°C , respectively.

Keywords: Composites, Solid electrolytes, Conductivity, XRD, DSC, SEM, EDX

1. Introduction

The demand for electronic products, such as laptop computers, mobile phones and electric vehicles has inevitably encouraged the research for higher-energy-capacity, lighter and safer lithium ion secondary batteries. The traditional liquid electrolytes such as aqueous batteries have many disadvantages. These batteries were reported to suffer from a number of major shortcomings such as limited temperature range of operation, device failure due to electrode corrosion by electrolytic solution and bulky in size. Thus to overcome these problems, solids exhibiting high ionic conductivity have been intensely studied.

The conductivity of composite solid electrolytes has been found to increase due to the influence of heterogeneous doping of insulating dispersoid in the host matrix [1]. The enhancement in the conductivity can be explained by various factors, depending on the physical and chemical properties of the composites. Among the mechanisms proposed are the space-charge layer effect [2], high concentration of point defect [3] and phase transition [4,5]. Recently, porous materials have been attracted by many researchers to be employed as composite solid electrolytes since they can provide large surface area between the host matrix and the dispersoid [6]. Composites with mesoporous oxides are the most synthesized and investigated [7,8,9]. The purpose of the present work is to prepare $\text{LiNO}_3\text{-Al}_2\text{O}_3$ composite solid electrolytes via water based sol gel method at a low temperature of 150°C . This method is inexpensive and simple. The structural and thermal properties of the composites are characterized by X-ray diffraction (XRD), differential scanning calorimeter (DSC), scanning electron microscopy (SEM) and energy dispersive X-ray (EDX) analyses. The dependence of their ionic conductivity on Al_2O_3 composition and temperature are investigated by AC impedance spectroscopy.

2. Experimental

The samples of the composite solid electrolyte are described by the general formula of $(1-x)\text{LiNO}_3-x\text{Al}_2\text{O}_3$ with $x = 0.1 - 0.5$ (mol percentage). The samples were prepared by sol gel method. Firstly, the starting host material, LiNO_3 (high purity grade) was dissolved in deionised water until a clear solution was obtained. The dispersoid powder of alumina, Al_2O_3 (high purity grade) was added to the solution and continuously stirred at a temperature of 40°C for 20 minutes. Next, the mixture was added to citric acid and heated at a temperature of 80°C on a hot plate with continuous stirring until a gel was formed. The gel was then heated at 150°C in an oven to dry. The sample was then crushed in an agate mortar to a fine powder. X-ray diffractograms of the composites were recorded on a D8 Advanced-Bruker X-ray Diffractometer. Calorimetric data were obtained using a METTLER TOLEDO DSC 822 with a continuous heating rate of $10^\circ\text{C min}^{-1}$. The morphology and chemical content were obtained using an INCA Energy 200 instrument (Oxford Ins.). The specific surface area and pore size were measured by a Brunauer–Emmett–Teller (BET) method. Conductivity studies were carried out on pellets pressed at a pressure of 6-8 tones/ cm^2 using a SOLATRON 1260 impedance analyzer at room temperature to 180°C over the frequency range of $10^{-1} - 10^7$ Hz.

3. Results and Discussion

3.1. Structure and Thermal Studies

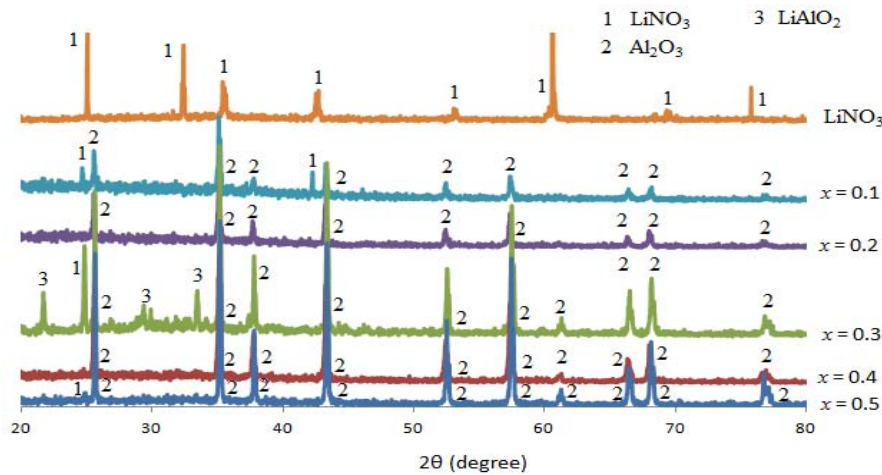


Fig. 1: X-ray diffraction patterns of pure LiNO_3 and $(1-x)\text{LiNO}_3-x\text{Al}_2\text{O}_3$ composites.

The XRD spectra of pure LiNO_3 and the $(1-x)\text{LiNO}_3-x\text{Al}_2\text{O}_3$ ($x = 0.1 - 0.5$) composites are shown in Fig. 1. The X-ray spectra of the composite samples show an amorphous characteristic of LiNO_3 as no crystalline peak of LiNO_3 appeared in the spectra. However, there are two peaks of a very low intensity of crystalline LiNO_3 appearing at $2\theta = 24.92$ and 42.26 for the composite sample with $x = 0.1$ followed by single peaks at $2\theta = 24.88$ and 24.98 for the composite samples with $x = 0.3$ and $x = 0.5$, respectively. The diffraction peaks at $2\theta = 25.72, 35.34, 37.90, 43.52, 52.68, 57.66, 61.08, 68.10$ and 77.00 in the spectra of the composite samples ($x = 0.1 - 0.5$) are attributed to the Al_2O_3 phase. A trace amount of a new phase is also detected in the diffraction pattern of the composite sample with $x = 0.3$. The presence of this new phase is indicated by additional reflections at $2\theta = 21.50, 29.00$ and 33.50 and is attributed to lithium aluminate, LiAlO_2 [10].

Fig. 2 displays DSC curves for composite samples with $x = 0.3$ to $x = 0.5$. The glass transition temperature, T_g at 80°C and the absence of melting point of crystalline LiNO_3 , indicate the presence of amorphous structure of LiNO_3 in the composite samples with $x = 0.4$. However, the crystalline characteristic of LiNO_3 with an amorphous background can be observed in the composite samples with $x = 0.3$ and 0.5 as indicated by the endothermic peak, due to the melting of crystalline LiNO_3 , T_m at 250°C and 252°C , respectively. The T_g of these composites is not clearly observed in the DSC curves. The exothermic peaks at $\sim 300^\circ\text{C}$ (for $x = 0.3 - 0.5$) are attributed to thermal decomposition of LiNO_3 [11].

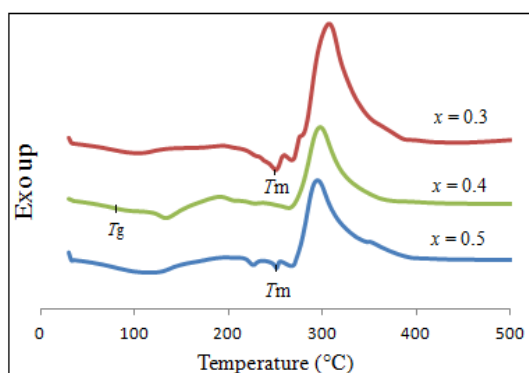


Fig. 2: DSC curves for $(1-x)\text{LiNO}_3-x\text{Al}_2\text{O}_3$ composites.

3.2. SEM, EDX and BET Analyses

The surface and cross-sectional SEM images of the composite sample with $x = 0.3$ are given in Fig. 3. Fig. 3(a) shows the structure of the amorphous phase of LiNO_3 as mentioned earlier. The surface SEM image also exhibits an excellent interfacial contact between the amorphous phases that spread over the alumina surfaces. The spreading of the amorphous phase provides a conducting pathway for Li^+ ions thus facilitates their transport in the composite. No agglomeration or isolation of alumina particles is observed and we can conclude that these insulating particles are homogeneously dispersed in the composite. As can be seen in Fig. 3(b), the composite sample exhibits a mesoporous structure of a type III isotherm according to the IUPAC classification. In this case, the composite has a mesoporous distribution and less of microporous type with the BET surface area of $55 \text{ m}^2 \text{ g}^{-1}$. However the porosity is low with pore sizes ranging from $\sim 1 \text{ nm} - \sim 5 \text{ nm}$. The mesoporous distribution due to the effect of sintering shows the interfacial interaction between the LiNO_3 and Al_2O_3 phases. This mesoporous structure ensures that the insulators are well dispersed in the composite ionic conductors such that both phases are interconnected three dimensionally [9]. Therefore, higher ionic conductivity can be expected in the composite due to the effect of larger surface area. The EDX analysis (Fig. 4) shows that Al, O and N are the major elements in the composite sample with $x = 0.3$. These elements could be attributed to the lithium nitrate (LiNO_3), alumina (Al_2O_3) and lithium aluminate (LiAlO_2), phases as discussed earlier.

3.3. Conductivity Study

Fig. 5(a) shows the compositional dependence of the ionic conductivity for $(1-x)\text{LiNO}_3-x\text{Al}_2\text{O}_3$ composites at room temperature. First, the conductivity increases with the Al_2O_3 content and then decreases after $x = 0.3$. The first phenomenon of the conductivity can be explained by the presence of a large surface area of contact between the host matrix and the dispersoid particles [12]. Consequently strong surface interaction of the ionic salt and oxide occurred and this led to the formation of amorphous phase of LiNO_3 as shown in Fig. 1. The effect of the crystal lattice disordering in the LiNO_3 ionic salt increases the number of mobile Li^+ ions in the composites thus enhancing the ionic conductivity [5]. The highest conductivity of $2.9 \times 10^{-4} \text{ S cm}^{-1}$ is obtained for the composite sample with $x = 0.3$ that can be related to the presence of a mesoporous structure as shown in Fig. 3. The conductivity decreases when $x > 0.3$. This is due to the limited number of host material (LiNO_3) to cover the alumina particles individually. Consequently, blocking effect on the transportation of Li^+ ions occurred due to the aggregation of the alumina particles.

Fig. 5(b) shows temperature dependence of the ionic conductivity for $(1-x)\text{LiNO}_3-x\text{Al}_2\text{O}_3$ composites at room temperature to 180°C . In general, the conductivity increases with temperature. At low temperatures, the curves of $\log \sigma$ versus $1000/T$ are non-linear. This phenomenon suggests that the samples are thermally activated and the state of the composites is gradually changing. At this temperature region (around T_g), the conductive ions are incorporated in glassy matrices and their mobility is lessened. The behaviour of the present system is similar to the family of lithium phosphate glasses reported by Kartini et. al [13]. However, starting from $\sim 120^\circ\text{C}$, the conductivity of the composites are seen to increase linearly with temperature and then, drop upon reaching $\sim 180^\circ\text{C}$. The observed phenomenon can be explained by the stability of LiNO_3 amorphous phase between $\sim 120^\circ\text{C}$ to $\sim 160^\circ\text{C}$ and melting of crystalline LiNO_3 slowly occurs near 180°C as indicated by the DSC curves in Fig. 2.

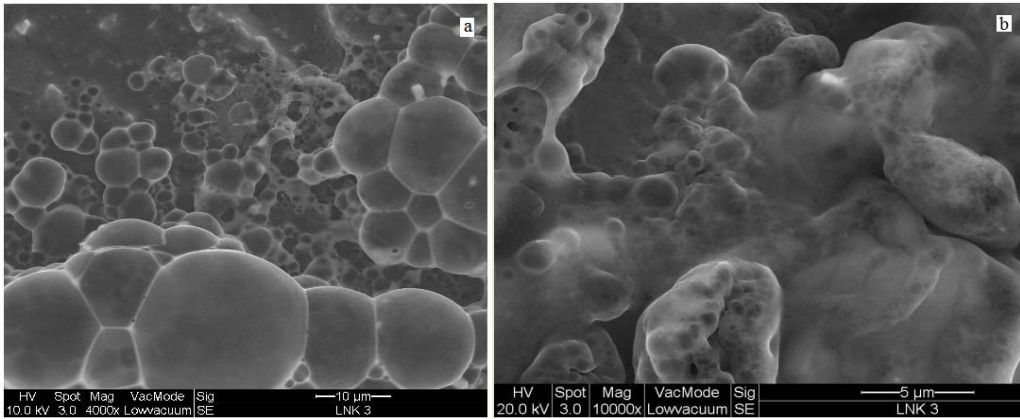


Fig. 3: SEM images of the composite sample with $x = 0.3$ (a) surface morphology and (b) cross section.

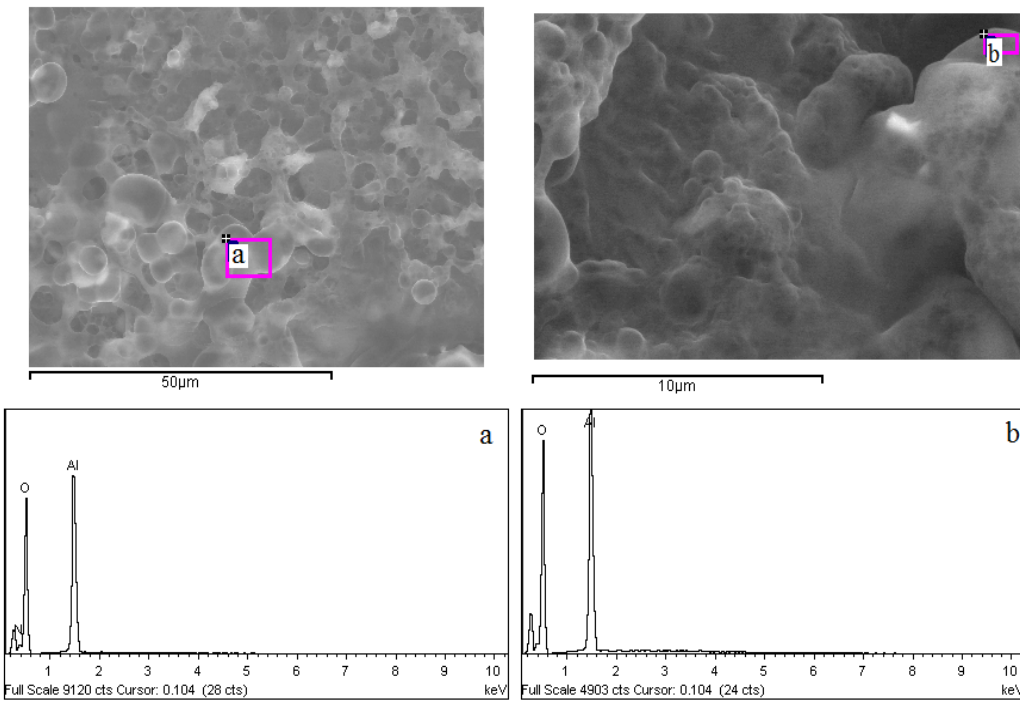


Fig. 4: EDX analysis of the composite sample with $x = 0.3$ at different points.

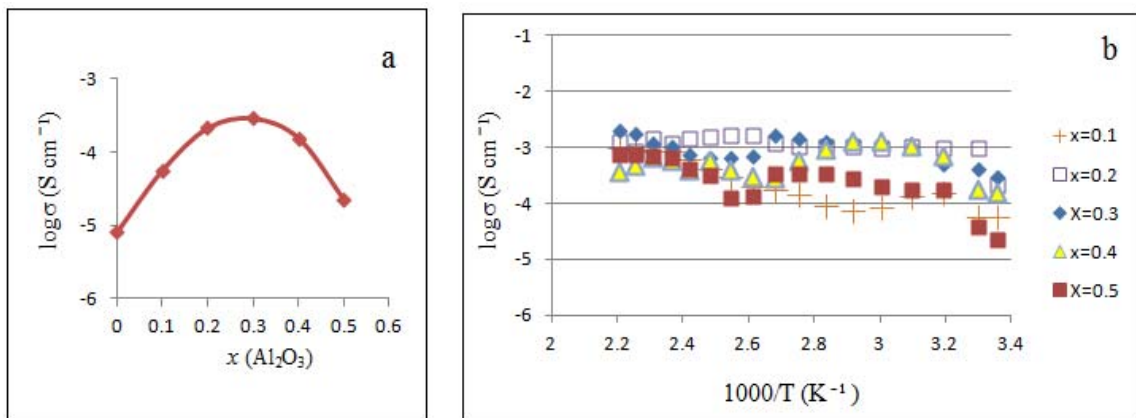


Fig. 5: Arrhenius plots of conductivity at room temperature (a) and $\sigma(x)$ dependences (b) for $(1-x)\text{LiNO}_3-x\text{Al}_2\text{O}_3$ composites.

4. Conclusion

In this work, the composite solid electrolytes in the system $(1-x)\text{LiNO}_3-x\text{Al}_2\text{O}_3$ were prepared by sol gel method. Structural, thermal, morphological and conductivity behaviours of the composites were investigated. XRD and DSC studies revealed that there is a formation of amorphous phase of LiNO_3 in the composite. A trace amount of a new phase of LiAlO_2 was detected in the composite sample with $x = 0.3$. The conductivity of the composites is likely to be due to the presence of the amorphous phase of LiNO_3 . The highest conductivity of $2.9 \times 10^{-4} \text{ S cm}^{-1}$ was obtained at room temperature for the composite sample with $x = 0.3$, that exhibited a mesoporous structure with a surface area of $55 \text{ m}^2 \text{ g}^{-1}$. The enhanced ionic conductivity is due to the effect of the large surface area.

5. Acknowledgment

The authors would like to thank the University of Malaya for awarding the Research Grant (RG021/09AFR) to support this work.

6. References

- [1] C.C. Liang. Conduction Characteristics of the Lithium Iodide-Aluminum Oxide Solid Electrolytes. *J. Electrochem. Soc.* 1973, **120** (10): 1289–1292.
- [2] J. Maier. Space charge regions in solid two-phase systems and their conduction contribution—I. Conductance enhancement in the system ionic conductor-‘inert’ phase and application on $\text{AgCl}:\text{Al}_2\text{O}_3$ and $\text{AgCl}:\text{SiO}_2$. *J. Phys. Chem. Solids* 1985, **46** (3): 309-320.
- [3] N.J. Dudney. Enhanced ionic conductivity in composite electrolytes. *Solid State Ionics* 1988, **28–30** (2): 1065-1072.
- [4] N.F. Uvarov, L.I. Brezhneva and E.F. Hairetdinov. Effect of nanocrystalline alumina on ionic conductivity and phase transition in CsCl . *Solid State Ionics* 2000, **136-137**: 1273-1277.
- [5] N.F. Uvarov, E.F. Hairetdinov, B.B. Bokhonov and N.B. Bratel. High ionic conductivity and unusual thermodynamic properties of silver iodide in $\text{AgI}-\text{Al}_2\text{O}_3$ nanocomposites. *Solid State Ionics* 1996, **86-88**: 573-576.
- [6] P. Knauth. Inorganic solid Li ion conductors: An overview. *Solid State Ionics* 2009, **180** (14-16): 911-916.
- [7] H. Maekawa, H.Y. Shen, Y. Fujimaki, K. Kawata, K. Shibata, M. Kawai and T. Yamamura. Mesopore Size Dependence of Protonic and Lithium Ionic Conductivity of Porous Alumina. *MRS Proceedings*, 835, K3.8, 2004.
- [8] H. Maekawa, R. Tanaka, T. Satoa, and Y. Fujimakia and T. Yamamura. Size-dependent ionic conductivity observed for ordered mesoporous alumina-LiI composite. *Solid State Ionics* 2004, **175**: 281–285.
- [9] H. Yamada, I. Moriguchi and T. Kudo. Nano-structured Li-ionic conductive composite solid electrolyte synthesized by using mesoporous SiO_2 . *Solid State Ionics* 2005, **176**: 945–953.
- [10] R.B. Khomane, A. Agrawal and B.D. Kulkarni. Synthesis and characterization of lithium aluminate nanoparticles. *Materials Letters* 2007, **61**: 4540–4544.
- [11] R.A. Ribeiro, G.G. Silva and N.D.S. Mohallem. The influences of heat treatment on the structural properties of lithium aluminates. *J. Phys. Chem. Solids* 2001, **62**: 857-864.
- [12] M.V.M. Rao, S.N. Reddy and A.S. Chary. DC ionic conductivity of $\text{NaNO}_3:\gamma-\text{Al}_2\text{O}_3$ composite solid electrolyte system. *Physica B*, 2005, **362**: 193-198.
- [13] E. Kartini, T.Y.S.P. Putra, I. Kuntoru, T. Sakuma, K.Basar, O. Kamishima and K. Kawamura. Recent studies on lithium solid electrolytes $(\text{LiI})_x(\text{LiPO}_3)_{1-x}$ for secondary battery. *J. Phys. Soc. Jpn.* 2010, **79** Suppl. A: 54-58.